**ELEKTRIKA**
Journal of Electrical Engineering

# Base Excitation Vibration Isolation Utilizing Magnetorheological Elastomer Models: A Simulation Study

**Thaer M. I. Syam**\*, **Asan G. A. Muthalif**, **Ayman M. H. Salem**, **Abdelrahman Ali** and **Yousif Badri**

Department of Mechanical and Industrial Engineering, College of Engineering, Qatar University, Doha, Qatar

\*Corresponding author: thaer@qu.edu.qa, Tel: +974-66641721

**Abstract:** Smart materials are those whose characteristics can be changed by external stimuli like temperature, pressure, and magnetic fields. Magnetorheological Elastomer (MRE) is a smart composite material made up of a polymer matrix with ferromagnetic particles incorporated in it. The interaction between the magnetic particles in an external magnetic field changes its mechanical characteristics, such as stiffness. The purpose of this article is to study the characteristics of several MRE models on a base motion isolation system. The loops of several MRE models from the literature, such as Bingham, Bouc-Wen, Modified Bouc-Wen, Dahl, and Hysteresis models, were simulated using SIMULINK and MATLAB on a base motion isolation (base excitation) system in this study. This is achieved by obtaining the time-domain results, and a 2nd order underdamped system analysis is used to study the behaviour and characteristics of the MREs. All these models are simulated, and their displacements with respect to time plots are obtained. The input signals that excite the base are a step and sinusoidal wave. Mathematical expressions identified Field-dependent parameters for each model are used form the literature. Results were analysed using the 2nd order underdamped system characteristics such as %PO, Tr and Ts. All of those parameters decreased when the applied current increases. Time-domain results reveal that as the current is increased, the damping is lightened and the stiffness is increased, due to the MRE's field-stiffening characteristics under a magnet field.

**Keywords:** Mathematical models, Magnetorheological elastomer (MRE), SIMULINK, Stiffness and damping, Time domain

## 1. INTRODUCTION

Mechanical vibrations are omnipresent in almost every machinery and are developed due to different external excitations. Such vibrations are undesired as it could lead to machinery breakdown and failures. The internal dynamics of the system and the external excitation force are two major aspects that affect the amplitude and frequency of any dynamic system in vibration [1]. The essential goal in vibration control is to reduce and isolate the vibration developed in machinery. There are different vibration isolation techniques which include: force isolation and motion isolation [2-3]. Analytical studies of base motion isolation are being conducted using various magnetorheological elastomer models (MRE).

MRE is a type of composite materials by which the ferromagnetic particles are embedded in a polymer matrix. Unlike magnetorheological fluids (MRF) which consists of a viscous fluid instead [5]. In the presence of a magnetic field, the magnetizable particles are arranged like a chain towards the direction of the field. Varying the magnetic field will affect the stiffness properties of the composite [3, 4].

Several applications such as vibration isolators, vibration attenuators, and dampers are based on the MRE due to it is properties [4]. Plenty of phenomenological

models have been implemented described by Hooke's and Newton's laws to deal with the viscoelasticity magnetorheological dampers [6,7]. One of the famous models to describe the MR damper viscoelasticity properties is the Bingham model. The material is assumed to be rigid before yielding [8]. The damping force, *F,* express the mathematical expression of this model:

$$F = f_c sgn(\dot{x}) + c_0 + f_0 \tag{1}$$

where $f_c$ the friction force due to yield stress, $c_0$ is the damping coefficient, $f_0$ is the stored force due to the accumulator.

Spencer et al. [4] developed a model that shows the hysteretic behavior of MR damper. This model resembles the characteristics and behavior of the damper. Therefore, it is more efficient than Bingham model. However, this model cannot fully describe the behavior of non-linear force concerning the velocity response at the yield region. The following mathematical equations can express this model:

$$F = \alpha z + c_0 \dot{x} + k_0(x - x_0) \tag{2}$$

$$\dot{z} = -\gamma |\dot{x}| z (|z|^{n-1}) - \beta \dot{x} |x|^n + A\dot{x} \tag{3}$$

where $\gamma, \beta, A$ and $n$ are Bouc-wen model parameters to control the hysteretic loop. $z$ is the deformation of the model due to the hysteretic effect represented by Equation (3), $\alpha$ is the scaling Bouc-Wen model parameter related to yield stress of MR damper, $k_0$ and $c_0$ are the spring stiffness and damping coefficient, respectively. $x_0$ is the initial displacement due to effect of the accumulator.

Similar to Bouc-Wen model, [4] adopted a 14-parameter model; the modified Bouc-Wen (MBW) model. This model considers the high non-linear behavior of MR damper as it enhances the accuracy of determining MR damper behavior. There is a limitation in this model due to the difficulty in approximating the high number of model parameters. The governing equations for this model are given by

$$F = c_1\dot{y} + k_1(x - x_0) \tag{4}$$

$$\dot{y} = \frac{1}{c_0 + c_1}[\alpha z + c_0\dot{x} + k_0(x - y)] \tag{5}$$

$$\dot{z} = -\gamma|\dot{x} - \dot{y}||z|^{n-1}z - \beta(\dot{x} - \dot{y})|z|^n + A(\dot{x} - \dot{y}) \tag{6}$$

where $\gamma, \beta, n$ and $A$ are modified Bouc-wen model parameters for controlling the hysteretic loop similar to the previous model. $k_1$ is the stiffness of the accumulator, $x_0$ is the initial displacement of spring $k_1$ due to accumulator effect, $z$ is an evolutionary variable. $y$ is the internal displacement of the damper, $c_1$ and $c_0$ are the viscous damping coefficients at low and high velocities, respectively.

Dahl model is one of the models developed to describe the behaviour of MR dampers. This model can be considered as a special case of the simple Bouc-Wen model with some differences in its parameters. The advantage of this model is that it reconstructs Coulomb forces to avoid the estimation of excessive coefficients [5]. The mathematical expression of this model can be expressed by

$$F = c_1\dot{y} + k_1(x - x_0) = k_0 x + c_0\dot{x} + \delta z - f_0 \tag{7}$$

$$\dot{z} = \rho(\dot{x} - |\dot{x}|z) \tag{8}$$

where $k_0$ is the stiffness of the spring, $c_0$ is the damping coefficient, $z$ is the intermediate variable, and $\rho$ is the coefficient of stiffness.

Yu et al. [6] proposed a new model that utilizes a hyperbolic sine function to represent the hysteresis to describe the stiffness and damping characteristics. This model can be expressed mathematically as follows

$$F = c_0 x + k_0\dot{x} + \alpha z + F_0 \tag{9}$$

$$z = sinh(\beta x) \tag{10}$$

where $\alpha$ is a factor to scale the hysteresis, and $k_0$ and $c_0$ are the spring stiffness and damping coefficient,

respectively. $F_0$ is the offset of the isolator force, $\beta$ is the scale factor of the displacement of the isolator,

Krauze and Kasprzyk [7] used Bouc-wen model as a semi-active suspension system and compared it to a passive suspension system, a quarter car model with two degrees of freedom body suspension wheels using MATLAB (Simulink). Results showed that using Bouc-Wen model as a semi-active damper improved. Soltane et al. [8] have used Bingham model to control cable vibrations. Desari et al. [9] introduced a novel method in estimating heart motion by applying MBW model to respiratory signals from a body. It is suggested that this model can be used as a robust unified framework to model hysteresis visualization in respiratory heart motion due to its accurate estimation. Augustynek and Urbas [10] studied the dynamic analysis of spatial linkages using Dahl model. This model was proposed and its parameters were identified using the modified artificial fish swarm algorithm [11], results of this model showed a satisfactory agreement with the experimental outcomes. Kamath and Wereley [12] presented and simulated several models numerically on the quarter-car suspension system in a vehicle. In addition, this study includes the passive vibration isolation approach. Simulations were run for four different excitation frequencies to mimic the roughness of the suspension system. Their results showed that Bingham and Bouc-Wen models behaved better than other models. A study by Syam and Muthalif [13] is done to observe their hysteresis behaviour and plot the transmissibility curves for base isolation for different MRE models. Results revealed that MBW and Dahl MRE models have an enhanced vibration levels reduction and isolation under a magnetic field.

In this article, time-domain results are obtained, and a 2$^{nd}$ order underdamped system analysis is used to study the behaviour and characteristics of the MREs. This is achieved by conducting simulation studies by using different MRE models such Bignham, Bouc-Wen, Modified Bouc-Wen, Dahl and Hysteresis on a base motion isolation (base excitation) system to understand the characteristics of MRE. MATLAB/SIMULINK software is used to model the methods using the block diagram scheme.

## 2. ANALYTICAL SIMULATIONS OF DIFFERENT MRE MODELS USING MATLAB/SIMULINK

### 2.1 Mathematical Model Development and Simulation Parameters

This work seeks to use MRE to control the parameters in semi-active vibration isolation. The system is presented as a simple movement isolation system (base excitement), which is used to isolate the excitation input to the base on the mass.

The mathematical modeling of the system is shown using the MRE models. The formulation of the mathematical modeling is described by equations using Conservation of energy and Newton's laws. One degree of freedom base isolation system is considered as shown in Figure 1.

An input displacement $y(t)$ is applied to the base as the

excitation and an output displacement *x(t)* on the mass is to be found. Five models are selected from the literature to be modelled and simulated on the base excitation system. Under a magnetic field, the properties of the MRE are altered. Mathematical representation for each model is presented based on their parameters which are field-dependent; this magnetic field is a function of the applied electric current. For each model, the simulation is conducted in the presence and absence of the MRE. In the absence of the MRE, the passive damping and stiffness are used. The current applied range is from 0 A to 4 A with an increment of 1 A.
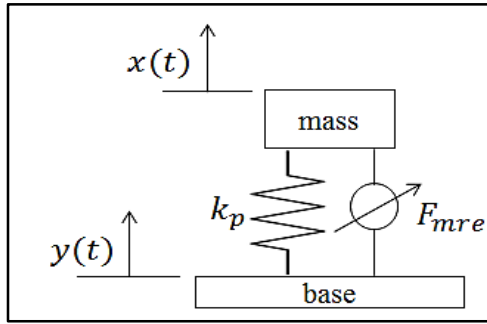


Figure 1. Schematic representation of base isolation model utilizing MRE.

The equation of motion is based on Newton law, and it becomes

$$\sum F = m\,\ddot{x} \qquad (11)$$

$$m\,\ddot{x} = -k_p(x - y) - F_{mre} \qquad (12)$$

$$m\ddot{x} + k_p x + F_{mre} = k_p y \qquad (13)$$

Knowing that the force of the MRE is given by

$$F_{mre} = k_{mre}(x - y) + [c_p + c_{mre}](\dot{x} - \dot{y}) \qquad (14)$$

Then, Equation. (14) becomes

$$\begin{aligned} m\ddot{x} + [c_p + c_{mre}]\dot{x} + [k_p + k_{mre}]x \\ = [c_p + c_{mre}]\dot{y} \\ + [k_p + k_{mre}]y \end{aligned} \qquad (15)$$

The dynamics of the system is illustrated using the equation of motion which is developed in terms of the input displacement, *y*, the output displacement, *x*, the mass, *m*, the passive damping coefficient and stiffness of MRE at 0 A, $c_p$ and $k_p$, the active damping coefficient and active stiffness of MRE under a magnetic field, $c_{mre}$ and $k_{mre}$. Since the damping properties are negligible for MRE, $c_p$ is not shown in Figure 1. The total MRE damping force $F_{mre}$ as in Equation. (14) includes the active damping coefficient. For simplification, let $c = c_p + c_{mre}$ and $k = k_p + k_{mre}$, therefore, Equation (15) becomes

$$m\ddot{x} + c\dot{x} + kx = c\dot{y} + ky \qquad (16)$$

In this study, the mass is assumed to be 5 kg. Table 1 depicts the parameters of the input signals. Moreover, MRE mechanical properties are varied under a magnetic field generated by applying an electrical current. The relationship of the properties variation with current is based on equations relating the models' parameters to the current, I. Those parameters can be constant or field-dependent. All of those relationships are picked from the literature and used in this study [11, 14–16].

Table 1. Excitation Inputs for the Analytical Simulations.

| Input signal | Parameters | Values |
|---|---|---|
| **Step** | Step time [s] | 0.5 |
| | Initial value [s] | 0 |
| | Final value [s] | 1 |
| **Sine wave** | Amplitude [m] | 1 |
| | Frequency [rad/s] | 10 |

The combination of the base isolation system and the damping force by these models is done by combining and processing the equations from Equations. (1) and (16). For instance, the mathematical expression for this methodology can be given as follows, reconsidering the Bingham model mathematical expression from Section 1, $F = f_c sgn(\dot{x}) + c_0 + f_0$, From Eq. (1), for base motion isolation system is

$$\ddot{x} = -\frac{k_{p_{Bingham}}}{m}(x - y) - \frac{F_{mre}}{m} \qquad (17)$$

By combining Equation (1) and Equation (13), and considering the relative motion between the mass output motion *x(t)*, and base input excitation *y(t)*, by which $x = (x - y)$ and $\dot{x} = (\dot{x} - \dot{y})$, the damping force of Bingham model is expressed by

$$F_{BinghamMR} = f_c sgn(\dot{x} - \dot{y}) + c_0 + f_0 \qquad (18)$$

The combination of the Bingham model damping force and the base isolation system becomes

$$\ddot{x} = -\frac{k_{p_{Bignham}}}{m}(x - y) - \frac{1}{m}(f_c sgn(\dot{x} - \dot{y}) + c_0 + f_0) \qquad (19)$$

The 2nd order differential equation form is most likeable to be built and implemented in SIMULINK using the block diagram. The block diagrams for all models are built. Equations (17-19) explain the formulation and combination of the base isolation and MRE models as a system.

The block diagram for the Bingham model on a base excitation system is shown in Figure 2.

MATLAB coding is coupled with the SIMULINK environment to simulate the systems. Two input signals are used a base excitation; step and sinusoidal waves, along with specific parameters shown earlier. All models were built on SIMULINK and gathered as subsystems so

that the simulations can be done in parallel for all models. Inputs were applied using a manual switch. The outcomes of those simulations are obtained on the scope as a time domain results, for both step and sine inputs. This is shown in Figure 3.
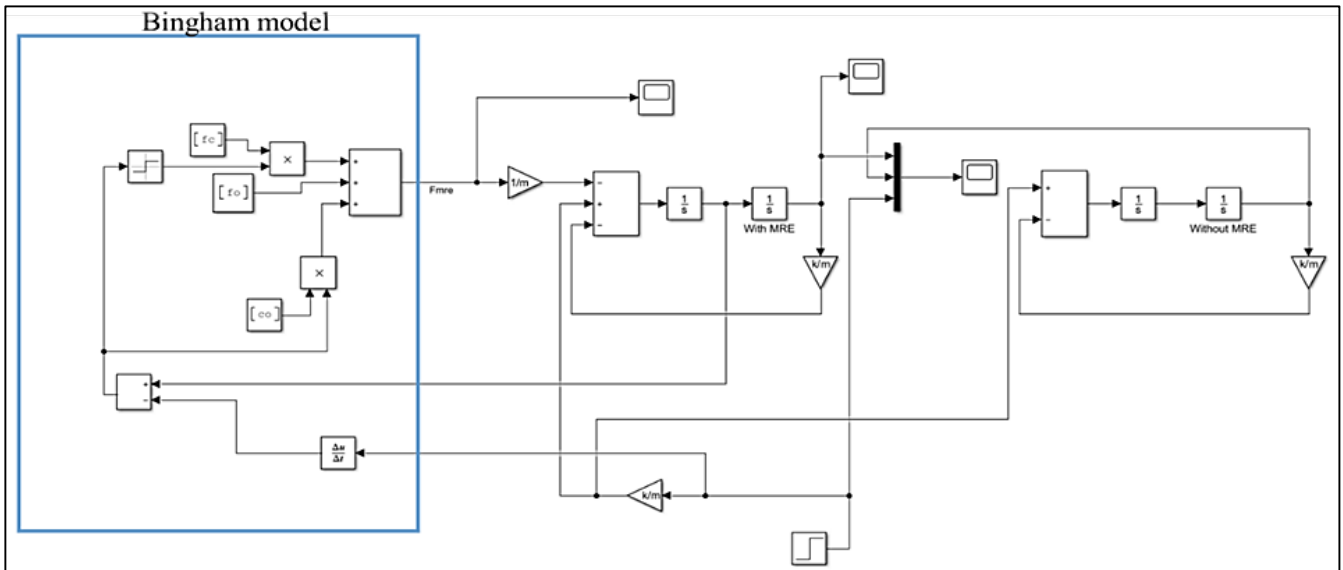


Figure 2. Block diagram for Bingham model on the base motion isolation system.
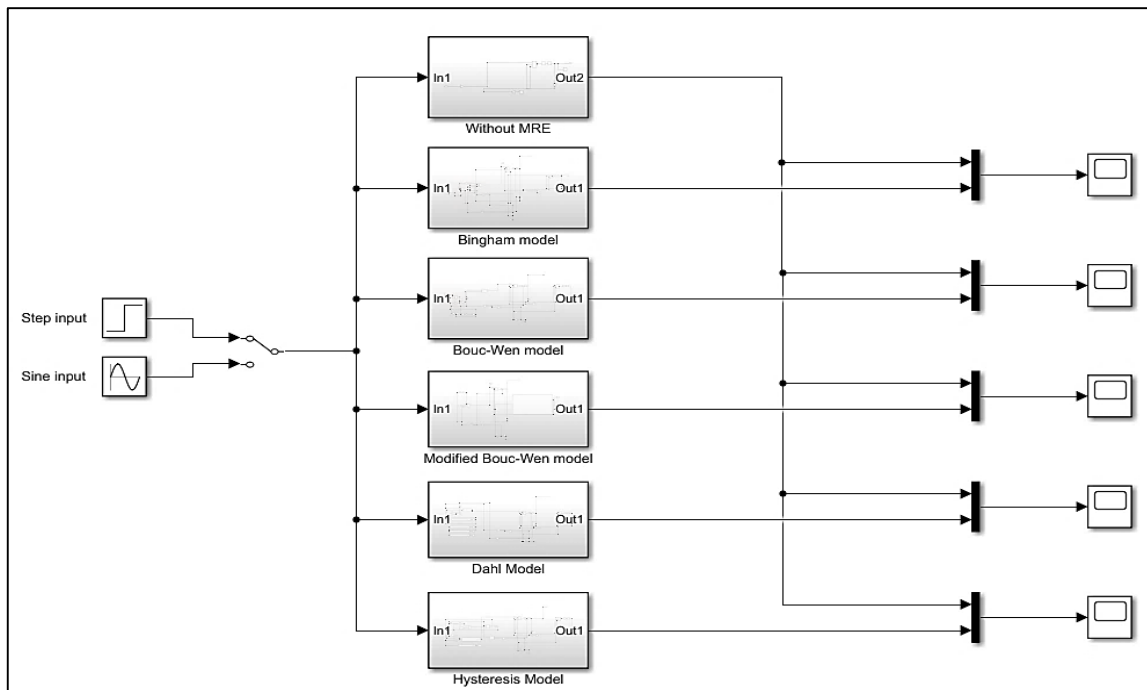


Figure 3. Simulink simulation as subsystems for different MRE models.

## 3. ANALYTICAL RESULTS AND DISCUSSION

Simulations were run, and all values of the parameters of the hysteresis semi-active MRE models were calculated at different values of current. These parameters, which are field-dependent, are mathematically expressed in the previous section.

All these models are simulated, and their displacements with respect to time plots are obtained. The input signals that excite the base are a step and sinusoidal wave as shown earlier. From the analytical simulations of these MRE models for semi-active base isolation system, it is vivid that as the current value increases, the damping and stiffness characteristics of MRE are enhanced and the vibration is reduced. Results of displacement to time are shown for each model with the two different excitations to the base. Results show that controlling the current from 0 A to 4 A significantly influences the behavior of MRE, a current of 0 A means that the damping force of MRE depends on the passive stiffness and damping. Results illustrate the response of the damped vibration system and the free vibration system for two excitation inputs: step and sine wave.

Simulation results for the five semi-active MRE base isolation models for two excitation inputs are shown in Figures (4-9), it can be clearly seen from the step input response that the damping is enhanced and more efficient

as the current increases. The mass is stabilized in a shorter time and the magnitude of the displacement is reduced. In addition, it can be concluded that for the sinusoidal responses, the displacement is reduced as the current is higher. From the step responses, when the applied current increases, the increase in the stiffness and damping properties of MRE is apparent as the displacement is reduced and the settling time decreases, which mean that the signal is reaching a steady-state faster. For example, this can be shown in a 'zoomed out' snapshot of the step response of the Bingham model (Figure 5).
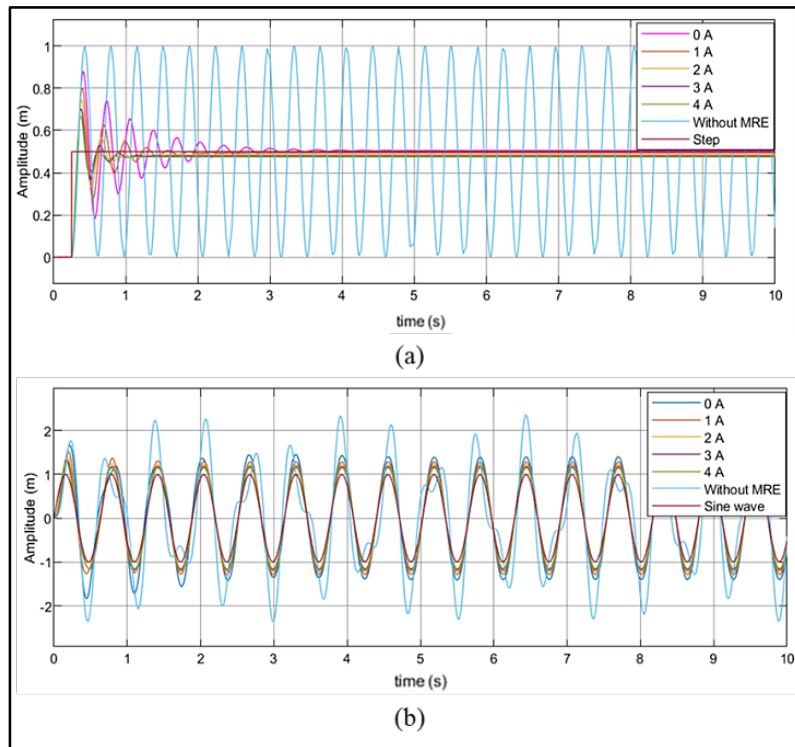


Figure 4. Amplitude vs time for Bingham Model excited by (a) step input, and (b) Sinusoidal input.
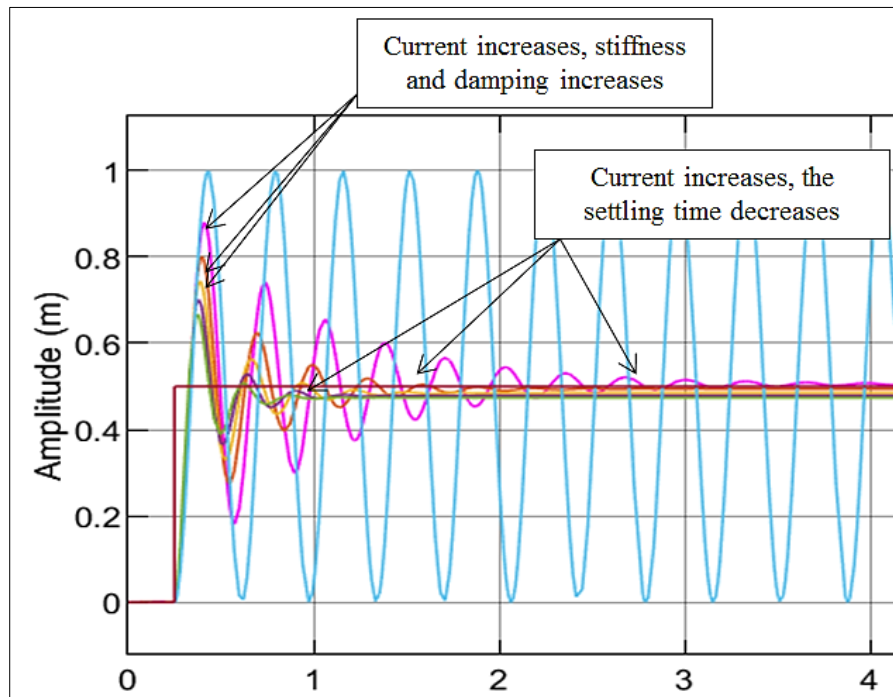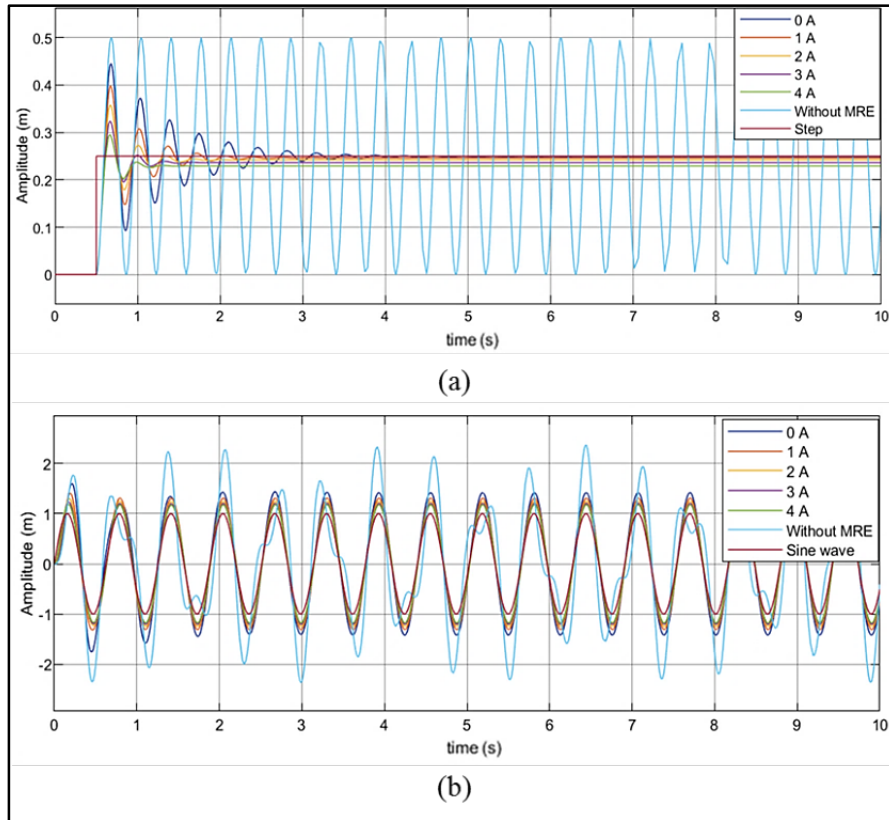


Figure 5. Zoomed out snapshot of Fig. 4 (a).

Figure 6. Amplitude vs time for Bouc-Wen Model excited by (a) step input, and (b) Sinusoidal input.
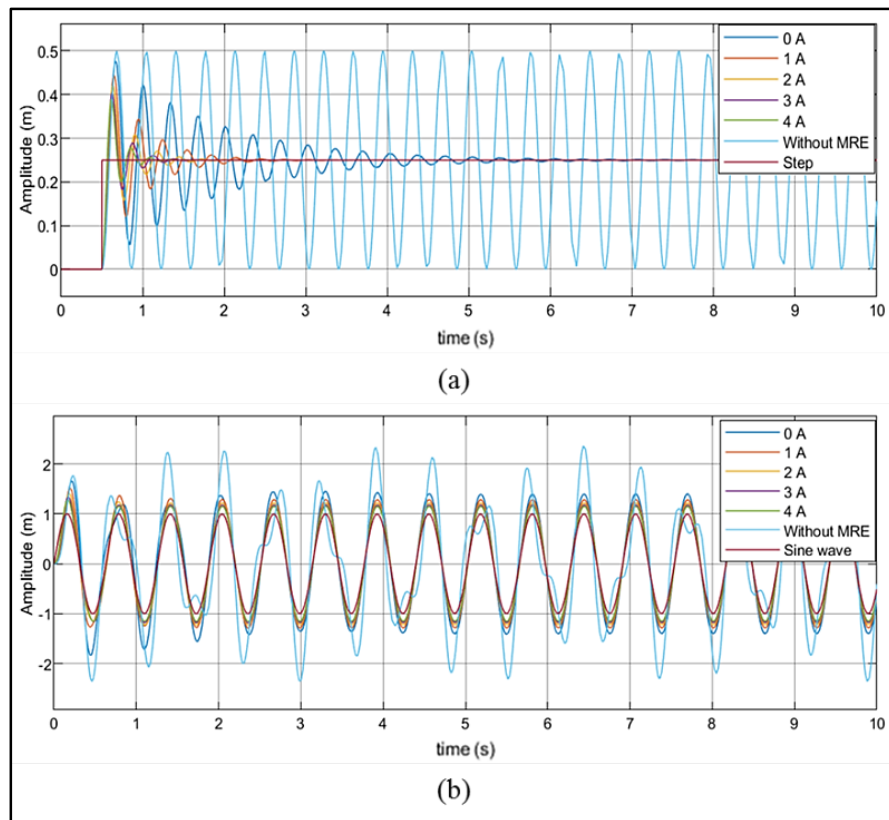


Figure 7. Amplitude vs time for MBW Model excited by (a) step input, and (b) Sinusoidal input.
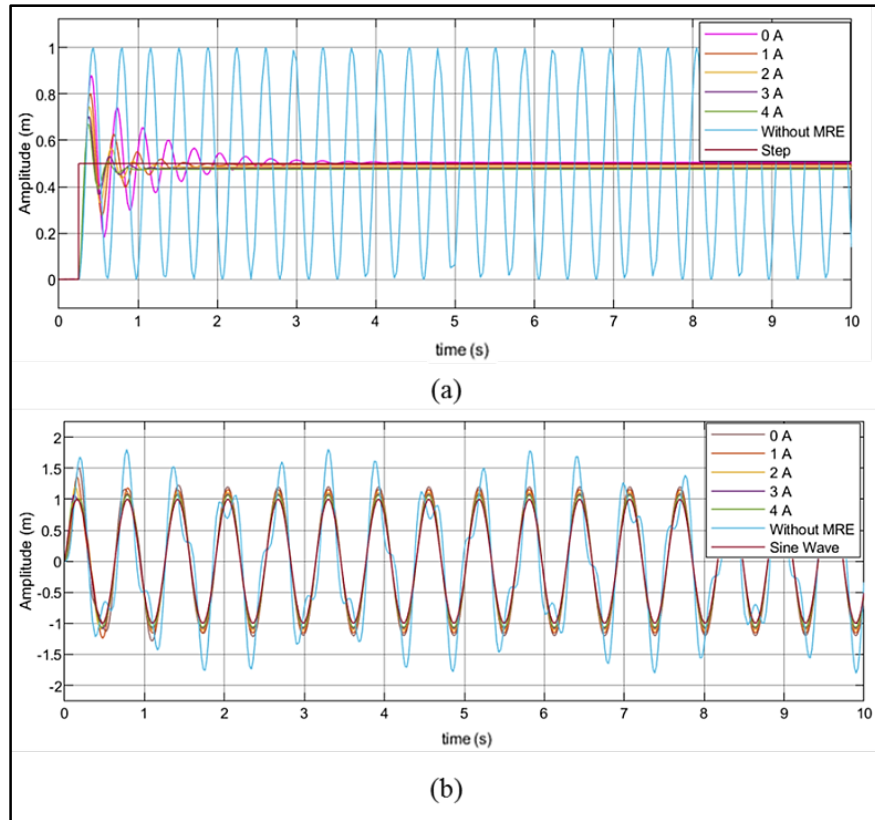
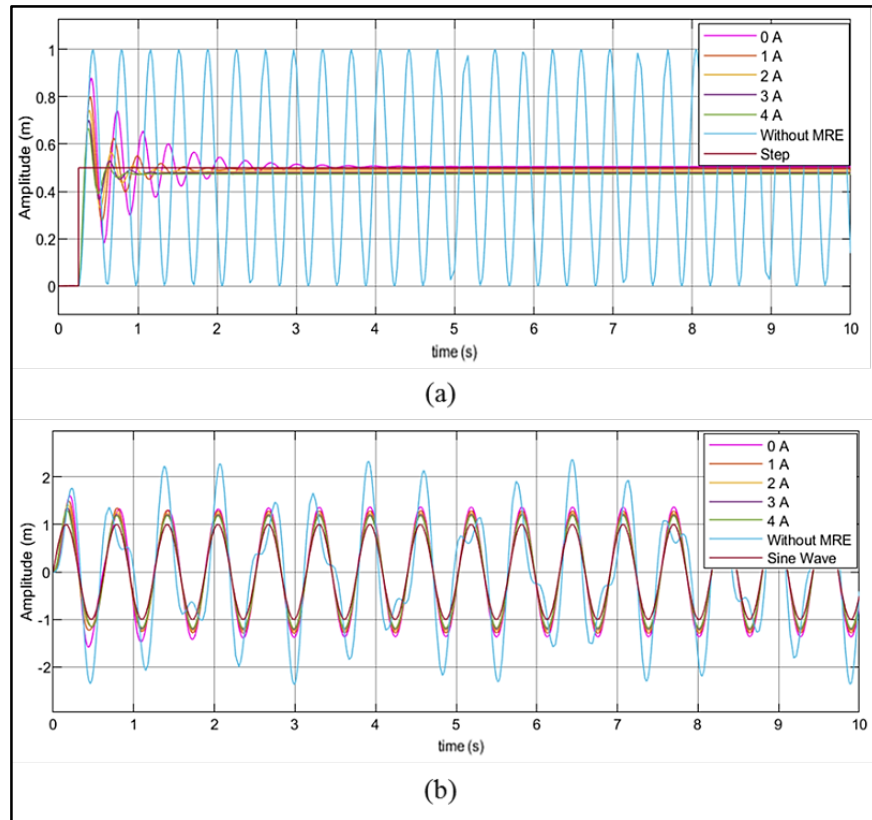Figure 8. Amplitude vs time for Dahl Model excited by (a) step input, and (b) Sinusoidal input.



Figure 9. Amplitude vs time for Hysteresis Model excited by (a) step input, and (b) Sinusoidal input.

To compare the damping characteristics of all models, Table 2 shows some parameters calculated by MATLAB software using property editor on figures such as $\%PO$, $Tp$ and $Ts$.

Table 2. Excitation Inputs for the Analytical Simulations.

| I | Bingham model | | | BW model | | | MBW model | | | Dahl model | | | Hysteresis model | | |
|---|---|---|---|---|---|---|---|---|---|---|---|---|---|---|---|
| | PO | Tp | Ts | PO | Tp | Ts | PO | Tp | Ts | PO | Tp | Ts | PO | Tp | Ts |
| [A] | % | [s] | [s] | % | [s] | [s] | % | [s] | [s] | % | [s] | [s] | % | [s] | [s] |
| 0 | 44.9 | 0.59 | 2.96 | 68.4 | 0.97 | 1.09 | 66.02 | 0.49 | 4.68 | 41.7 | 0.54 | 0.68 | 41.6 | 0.63 | 0.79 |
| 1 | 39.5 | 0.52 | 2.23 | 53.4 | 0.77 | 0.72 | 63.9 | 0.30 | 2.68 | 38.2 | 0.39 | 0.47 | 38.1 | 0.45 | 0.55 |
| 2 | 34.2 | 0.48 | 1.79 | 44.7 | 0.73 | 0.55 | 63.8 | 0.25 | 2.18 | 34.7 | 0.32 | 0.38 | 34.7 | 0.37 | 0.45 |
| 3 | 31.3 | 0.43 | 1.49 | 40.0 | 0.71 | 0.43 | 59.7 | 0.23 | 1.75 | 31.4 | 0.28 | 0.33 | 31.4 | 0.33 | 0.38 |
| 4 | 26.7 | 0.42 | 1.28 | 33.6 | 0.69 | 0.38 | 49.3 | 0.20 | 1.12 | 28.3 | 0.26 | 0.29 | 28.2 | 0.30 | 0.34 |

For the Bingham model, the %$PO$ values are reduced as the current increases. For example, the %$PO$ values are 44.922% and 39.472% when the applied current values are 0 A and 1 A, respectively. This shows that the displacement amplitude is being reduced. In addition, $Tp$ is reduced in each iteration which means that the time needed to achieve the peak displacement is decreasing; this illustrate that the response tends to shift, and the natural frequency of the system is increasing. This shift in the natural frequency is a sign that the vibration is being reduced with the current. To prove this, the settling time for all iterations was calculated and shown in Table 2. The settling time is reduced from 2.959 s to 1.281 s as the current increases from 0 A to 4 A. This means that the time needed for the oscillation to achieve ±2% steady-state value. Therefore, the vibration is reduced, and the steady-state value is achieved in lesser time.

This conclusion is shown clearly for all other four models (BW, MBW, Dahl and hysteresis). Vibration is reduced as the MRE is exposed to more current, more magnetic field. BW model showed a reduction in the %PO from 69.378% to 33.654% as the current increases from 0 A to 4 A. Tp and Ts are reduced as well, meaning that the natural frequency is being increased and the vibration reduction is greater, similarly to MBW, Dahl and Hysteresis semi-active MRE models. The mass of the system is constant, which is assumed to be 5 kg. All other models' parameters are changeable and depend on the current. In terms of $Ts$, the lowest time needed for the oscillations to be steady for the passive stiffness and damping (0 A current) is 0.676 s for the Dahl model, and it kept decreasing as the current increases. This shows that vibration reduction is superior for this model other than other models.

In contrast, the maximum value for $Ts$ for the passive MRE properties is shown in MBW model (4.682 s and kept decreasing). This means that the underdamped oscillation took much time in reaching the steady-state value. This is due to the complexity of MBW model as it includes 14 parameters that control its hysteresis loop.

## 3. CONCLUSION

For the basic motion isolation system, the mathematical model was developed in combination with the mathematical model of five distinct MREs for step and sinusoidal excitement inputs. In the analytical simulation study, it can be determined that the vibration in the base isolation system was reduced by various MRE models. Simulink and MATLAB have been used for Bingham, Bouc-Wen, Modified Bouc-Wen, Dahl and Hysteresis loops modelling. Mathematical expressions identified Field-dependent parameters. Results showed that the damping is being lightened when the applied current increases, this is due to the field-stiffening properties of the MRE under a magnetic field. In addition, a shift in the time domain responses is observed, meaning that the stiffness is changed. Results were analysed using the 2nd order underdamped system characteristics such as %PO, Tr and Ts. All of those parameters decreased when the applied current increases. This concludes that the system is being isolated since the time needed for the response to be steady is less. It can be expected that the system's natural frequency will increase each time, hence reducing the vibration levels. This article reviewed various MRE models and studied their effectiveness in vibration isolation on a base excitation system. The main goal of this study was to test the performance of different MRE models using the time domain analysis and properties under an external magnetic field. Results presented in this paper can be improved to be used in the transmissibility analysis, and the shift in it is graph which is an essential concept in vibration isolation. Also, this simulation can be done on a quarter car model in a vehicle to investigate the ability of using such models in the suspension system dampening. In addition, an engine mount system can be a promising application where those models can be used in.

## REFERENCES

[1]  H. Wen, J. Guo, Y. Li, Y. Liu, and K. Zhang, "The transmissibility of a vibration isolation system with ball-screw inerter based on complex mass," *J. Low Freq. Noise, Vib. Act. Control*, vol. 37, no. 4, pp. 1097–1108, Dec. 2018.

[2]  T. Syam, A. Muthalif, A. Salem, and A. Hejazi, "3D numerical modelling and analysis of a magnetorheological elastomer (MRE)," *J. Vibroengineering*, pp. 1–15, 2020.

[3]  T. M. Syam, A.. Hegazi, A. Muthalif, & Y. Badri (2021). Magnetorheological Elastomer-Based Variable Stiffness Flexible Coupling for Vibration Isolation. *Transactions of the Canadian Society for Mechanical Engineering*. https://doi.org/10.1139/tcsme-2021-0007

[4]  B. F. Spencer, S. J. Dyke, M. K. Sain, and J. D. Carlson, "Phenomenological Model for Magnetorheological Dampers," *J. Eng. Mech.*, vol. 123, no. 3, pp. 230–238, Mar. 1997.

[5]  Y. Badri, T. Syam, S. Sassi, M. Hussein, J. Renno, & S. Ghani (2021). Investigating the characteristics of a magnetorheological fluid damper through CFD modeling. *Materials Research Express*, *8*(5), 055701. https://doi.org/10.1088/2053-1591/abfcf6

[6] Y. Yu, Y. Li, and J. Li, "A new hysteretic model for magnetorheological elastomer base isolator and parameter identification based on modified artificial fish swarm algorithm," *31st Int. Symp. Autom. Robot. Constr. Mining, ISARC 2014 - Proc.*, no. Isarc, pp. 176–183, 2014.

[7] P. Krauze and J. Kasprzyk, "Vibration control in quarter-car model with magnetorheological dampers using FxLMS algorithm with preview," in *2014 European Control Conference, ECC 2014*, 2014, pp. 1005–1010.

[8] E. C. Bingham (1916). An investigation of the laws of plastic flow. *Bulletin of the Bureau of Standards*, *13*(2), 309. https://doi.org/10.6028/bulletin.304

[9] P. K. R. Dasari *et al.*, "Adaptation of the modified Bouc-Wen model to compensate for hysteresis in respiratory motion for the list-mode binning of cardiac SPECT and PET acquisitions: Testing using MRI," *Med. Phys.*, vol. 41, no. 11, Nov. 2014.

[10] K. Augustynek and A. Urbaś, "Comparison of bristles' friction models in dynamics analysis of spatial linkages," *Mech. Res. Commun.*, Apr. 2016.

[11] Y. Yu, Y. Li, and J. Li, "Parameter identification of a novel strain stiffening model for magnetorheological elastomer base isolator utilizing enhanced particle swarm optimization," *J. Intell. Mater. Syst. Struct.*, vol. 26, no. 18, pp. 2446–2462, Dec. 2015.

[12] G. M. Kamath and N. M. Wereley, "A nonlinear viscoelastic-plastic model for electrorheological fluids," *Smart Mater. Struct.*, vol. 6, no. 3, pp. 351–359, 1997.

[13] T. M. I. Syam and A. G. A. Muthalif, "Hysteresis behaviour of different magnetorheological elastomer models: Modelling and simulation," *Vibroengineering Procedia*, vol. 31, pp. 7–14, 2020.

[14] X. Zhu and X. Lu, "Parametric identification of Bouc-Wen model and its application in mild steel damper modeling," in *Procedia Engineering*, 2011, vol. 14, pp. 318–324.

[15] M. K. M. Razali, A. G. A. Muthalif, and N. H. D. Nordin, "Estimation of Parameter for Different Magnetorheological Fluids Model for Varying Current," *Int. J. Comput. Electr. Eng.*, vol. 10, no. 2, pp. 127–134, 2018.

[16] Y. Yu, Y. Li, and J. Li, "Parameter identification and sensitivity analysis of an improved LuGre friction model for magnetorheological elastomer base isolator," *Meccanica*, vol. 50, no. 11, pp. 2691–2707, Nov. 2015.